

Flow Separation Modes and Side Phenomena in an Overexpanded Nozzle

Vladeta Zmijanović

Graduate student
Fluid Mechanics and Energetics
École Polytechnique

Boško Rašuo

Full Professor
University of Belgrade
Faculty of Mechanical Engineering

Amer Chpoun

Full Professor
Université Evry Val d'Essonne
Laboratoire de Mécanique et d'Energétique
Evry (Paris region), France

As a part of an aerodynamics Ecole Polytechnique project, separation modes which occur in supersonic nozzles at overexpanded regimes are numerically investigated and compared with known effects. Different shock generation and reflections in different nozzle types are observed and their impact on the two main separation modes, namely Free and Restricted Shock Separation (FSS & RSS) is explored. ONERA' experimental thrust-optimized-contour (TOC) rocket nozzle was the reference case and it is compared with the corresponding Vulcain 2 nozzle and analogues conical and TIC nozzle contours. Strong lateral forces and side effects on the nozzle wall caused by the RSS and by transition FSS to RSS are depicted in terms of flow unsteadiness and presented in flow charts and diagrams. Additionally, some design criteria for modern thrust optimized nozzles according to these effects are proposed.

Keywords: launcher nozzle, TOC, TIC, conical contour, overexpanded regime, free, restricted shock separation.

1. INTRODUCTION

The nozzle, an end-element of the propulsive process cycle, represents a critical part of any aerospace vehicle. The task of accelerating and efficiently exhausting combusted and reactive gases according to the delivered thrust represents the main objective of the propulsion system design. As such, propulsive convergent-divergent (C-D) axisymmetric rocket nozzles have evolved since the early period of use till nowadays. From technical and historical point of view, it is possible to sort axisymmetric nozzle types by the shape of their divergent profile as conical, ideal - de Laval, truncated ideal contour (TIC) and sorts of modern thrust optimized contour (TOC) nozzles.

In the space launcher engine design it is of substantial importance to optimize and control flow end-effects at the conventionally used nozzles. The launcher nozzle, designed to work in extremely wide range of pressure regimes has critical stress points at its lower and upper limits of operation envelope. With the high ambient pressure and thus, lower nozzle pressure ratio (NPR) than the designed one, exhaust plume is over-expanded and it is being recompressed through the shock reflections to the ambient pressure. The nozzle flow under certain circumstances generates critical side-loads on the walls. This mainly occurs when the flow is separated due to an overexpansion and during the start-up transition processes. Different types of flow separation are possible with the different nozzle types as well within the same nozzle. At largely over-expanded regime boundary-layer is detached from the nozzle wall due to an adverse pressure gradient generating the

separation shock. This supersonic and separated flow continues downstream and it may interact with the recompression shocks, asymmetric jet portions and/or possibly present internal shock, which can further lead to the severe lateral loads. These lateral or side-loads of uncontrolled flow separation are frequently present during the transient processes of engine start-up and shut-down operation. As the part of the Ecole Polytechnique applied aerodynamics student-project under the guidance of ONERA, the separation effects and nature of such produced flow field are investigated.

2. STATE OF THE ART OF THE PROBLEM IN BRIEF

The presented study is motivated by the flow and performance investigations of the contemporary nozzles used in the space launcher technology. This implies use of the thrust optimized and compressed parabolic nozzles. The main reasons for the use of these nozzles are higher thrust performance on the shorter nozzle divergent section length and thus the smaller mass of the launcher propulsion system.

Following the principles of the shockless de Laval ideal nozzle, whose contour may be also numerically obtained in respect to the method of characteristics (MoC) procedure [1], it is possible to further optimize this contour in the direction of thrust to mass ratio. Optimization of the ideal nozzle would consider subsonic and supersonic throat section curvature radius but still with a smooth transition and calculation according to Kliegel, Sauer or another method of sonic line as an incipient point for further MoC calculation process. The calculated divergent supersonic profile with marching characteristic until the completely parallel Odeg and uniform exit flow in the first optimal derivation may be truncated according to the maximum delivered thrust. In the usual design process optimal exit angle of the truncated ideal contour (TIC) nozzle profile is found between 4.5 and 7.5 deg but its naturally

Received: September 2009, Accepted: June 2012
Correspondence to: Vladeta Zmijanović
École Polytechnique,
91128 Palaiseau cedex, France
E-mail: vladeta.zmijanovic@polytechnique.edu

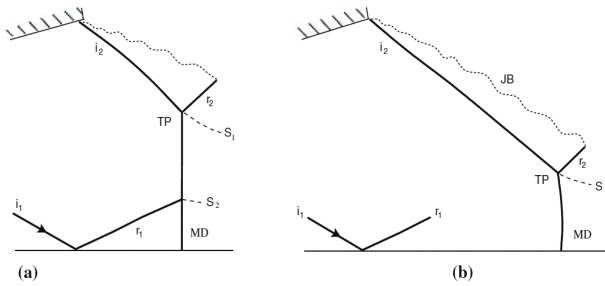


Figure 1. Schematic illustration of shock interaction near the nozzle lip for two pressure ratios by Hadjadj, Onofri [2]

depends on the designed nozzle pressure ratio NPRD. After truncation, the nozzle parallelism and uniformity at the exit section is lost but still there is no shock appearing inside the nozzle. Additional optimization from this point includes further shortening of the divergent contour either by compressing the TIC contour or by calculating profile, changing the marching characteristic in MoC with the optimization criterion (max delivered thrust). With number of improved characteristic TOC nozzle exhibits the additional effects that need to be taken into account namely, an internal shock which is discussed further.

2.1 Nozzle flow patterns

The nozzle plume out of the nozzle recompresses to the ambient pressure through the recompression and consequent shock waves. The interaction of these shock waves forms characteristic patterns dependent on the flow conditions and the nozzle contour type. As nozzle is adapted to best perform at certain pressure ration derogation from this value will lead to over or under expansion flow regime. Underexpansion is usually less detrimental in performance terms than overexpansion. Therefore, the nozzle operation envelope is designed accordingly but it is also dependent on specific mission objectives and in which flight segment the highest performance is necessary.

Several distinguishable flow patterns of an overexpanded nozzle jet plume are considered in this study; regular shock reflection, the Mach reflection and the cap-shock pattern. The first two shock interactions patterns, regular and Mach reflection (MR) are present in all conventional axisymmetric CD nozzle types.

The over expanded flow regime, when pE is lower than p_a , a shock wave and a deflection of the jet line corresponding to a contraction of the jet form at the exit lip. Compression surrounded by the shock surface ends with the Mach disk. The slope gradient depends highly

on the pressure ratio and thus on the height or size of the Mach disk. In Figure 1 two cases of full and over flowing nozzle regimes are depicted. It is observable that for given pressure ratios only classical Mach reflection is possible. Decrease of an ambient pressure or increase of a chamber pressure results in Mach disk size reduction and detrimental slope angle. Further pressure ratio increase will result in farther downstream displacement of the Mach disk and reduction in size until smooth transition from a MR to an apparent regular reflection (aRR) as denoted by Hadjadj and Onofri [2].

The regular reflection (RR) solution in axisymmetric flows, discussed here, is theoretically impossible. This stage of the shock reflection is transitional and represents a limiting case, where one compression sequence ends without Mach disk on the end, as in Figure 8. This limit is questionable since it is a matter of observation which size of the Mach disk is small enough to be neglected. The case with infinitesimal Mach disk size is denoted as an apparent regular reflection, aRR.

Apart from the classical Mach and regular reflection configurations, there is a third pattern conventionally denoted as the cap shock. The cap shock pattern is closely related to the nozzles with internal shock as thrust-optimized-contour nozzles, parabolic and compressed TIC nozzles. Nevertheless, in Figure 2a represented Mach reflection with inside curved Mach disk cap shock form but it is not originating from the internal shock reflection but from the strong overexpansion caused upstream nonuniformities. This is characterized by the strong vortical pressure gradient. In Figure 2 b and c conventional caps shock pattern is formed mainly due to the impingement of the internal shock with the central Mach disk. The reflected shock from this interaction meets later with the incident shock which originates from the boundary layer separation and they form either regular reflection as in b or Mach reflection as in the case c, depending on their respective slopes. Nozzles with present internal shock may have compression sequence with any of the three mentioned shock reflection configurations. The transition from the Mach reflection to the cap shock pattern appears for certain pressure ratios where boundary layer rapidly separates from the nozzle wall and when Mach disk is close enough to the nozzle exit that it can interact with the internal shock. Otherwise, if Mach disk is distant the cap shock pattern will not occur but only Mach reflection or aRR, Figure 1.

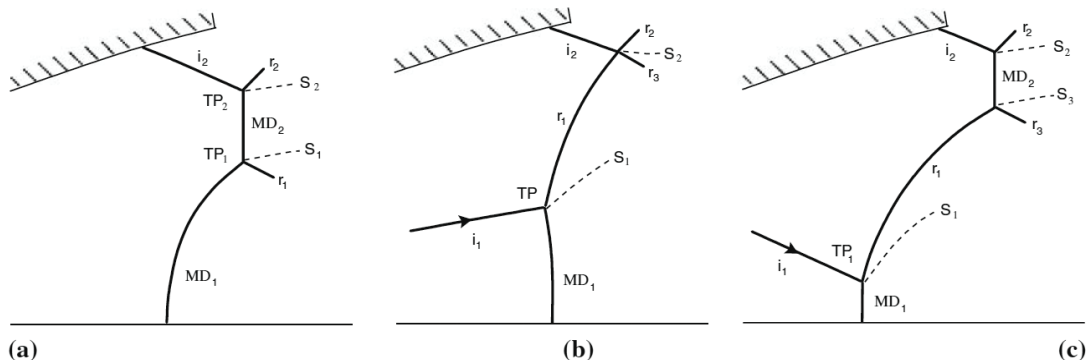


Figure 2. Schematic illustration of shock interactions and cap shock pattern in overexpanded supersonic nozzles, [2]

2.2 Separation patterns

When pressure ratio is pushed further from the designed one, either at highly overexpanded nozzles or in transitional phase when full flowing is not still established, flow violently separates from the nozzle wall upstream due to an adverse pressure gradient. The separated boundary-layer flow continues as a free jet and exits the nozzle. This separation mode named as free shock separation (FSS) was observed early as, reported in number of empirical models in the late '50s and '60s and it is well understood till now. With the further development of the high power nozzles, namely TOC and compressed parabolic as for example of J-2S engines asymmetric FSS has been reported and investigated. In the '70s during the cold flow tests of the J-2S, Nave and Coffey [3] first reported the phenomenon of asymmetric flow separation that yields tilted separation surface and causes highest value of the side loads. Particularly, pressure downstream of the separation showed unsteady behavior with the strong oscillations and values quite above the ambient one which they attributed to the reattachment of the separated flow to the nozzle. Since the separation extension is limited by this, they named it restricted shock separation (RSS).

The same behavior is noted during the development of the contemporary used TOC launcher nozzles as Vulcain 2 nozzle and reported in works as of Hagemann and Frey [4-6], Deck [7], Reijasse [8], Schimizu et al. [9], Roquefort [10]. Hagemann and Frey [4] related the RSS problem with the internal shock and cap shock pattern which, as mentioned, are characteristic for the TOC and compressed parabolic nozzles. The strong side loads due to RSS are one of the major concerns of the modern launcher rocket engine design. In the current study, TOC nozzle is investigated for pressure ratios under which FSS, RSS and shock patterns occur at hysteresis regime.

3. NUMERICAL SIMULATION ENVIRONMENTS AND TEST MODELS

The code based on the method of characteristics, briefly described in Section 2, is used to design truncated ideal contour nozzle and simplified MoC method for the corresponding conical nozzle. These nozzles served as the comparison and identification test cases to complement results of the Rao [11] TOC nozzle model. Predesigned by ONERA, TOC nozzle model basic properties are listed in Table 1.

Table 1. Design parameters of the ONERA TOC test nozzle

Throat radius	$r_t=0.01362\text{ m}$
Divergent section length	$L=15r_t$
Area-expansion ratio	$E=A_{exit}/A_t=30.32$
Exit Mach number	$M_{exit}=5.243$
Designed nozzle pressure ratio	$NPR_D=p_c/p_a=657.9$

The TOC nozzle together with comparison models is confronted to the range of different pressure ratios in order to identify and describe flow patterns. In the investigation, structured mesh with hexagonal elements

is used. Basic axisymmetric two-dimensional (2D) mesh of the nozzle region consisted of 275 nodes in the axial direction and 114 in vertical direction which were clustered toward the nozzle wall and the throat section.

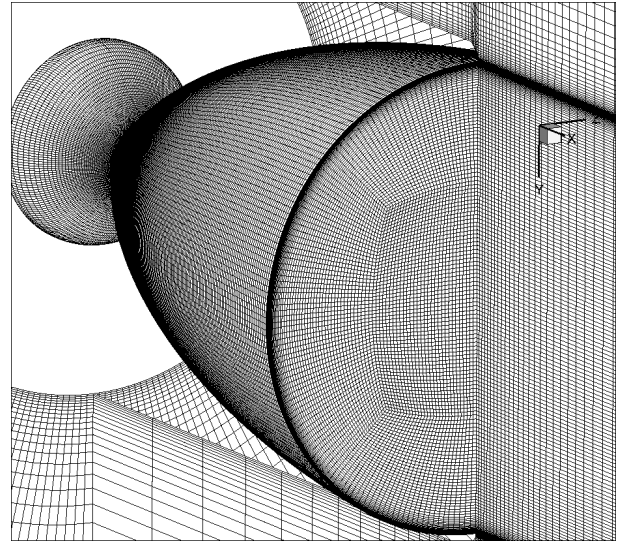


Figure 3. 3D numerical grid of the TOC test nozzle

This mesh was further improved with higher resolution grid of 300x200 obtaining y^+ between 1.3 and 3.7 at adapted flow regime. In order to illustrate the behavior and unsteadiness in the three-dimensional domain, full 3D numerical grid was composed with 8.2 million of hexagonal elements (6.6 million in the nozzle region).

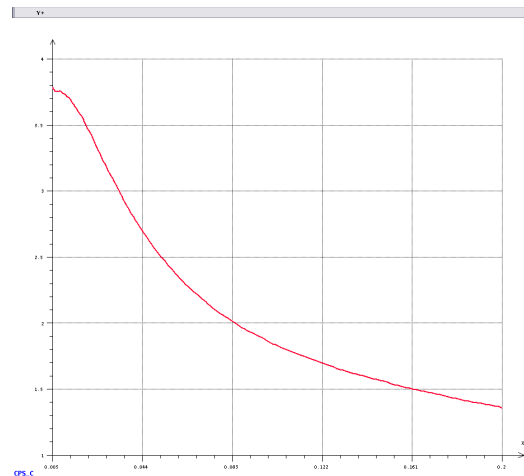


Figure 4. y^+ at divergent section wall boundary

3.1 elsA CFD code environment

The 2D axisymmetric calculations were performed on the structured finite volume solver of ONERA code *elsA* 3.1.15 (ensemble logiciel de simulation en Aérodynamique) [12] by solving in first step Euler and then averaged compressible Navier-Stokes equations. The *elsA* project [12] has begun in 1999, by ONERA, CERFAX and Airbus France from number of different codes and since then it has evolved from a CFD code to the complete multidisciplinary software package. Alternatively to the conventional codes, *elsA* is written in C++ with linkage to the FORTRAN routines for process demanding operations, while the GUI is in the

python. It was aimed for compressible and complex geometries internal and external flows and it includes internal and external flow Euler, RANS, URANS, DES and LES CFD structured solvers as well simulation software for aeroelasticity, aerothermics coupling, aeroacoustic coupling etc.

In the current study Euler and RANS are used for the axi-2D nozzle flow simulation and RANS for the nozzle with coupled external domain simulation.

3.2 CPS_C CFD code environment

Code pour la Propulsion Spatiale cryo (CPS_C) is the finite volume compressible unstructured CFD code aimed at reactive space propulsive flows. It includes Favre averaged Navier-Stokes (FANS) solver as well detached and large eddy simulation DES and LES solvers. CPS code is developed by the French center for space investigation CNES, Bertin[©] and SNPE [13], [14] in 1999 as an unified code for space propulsion and it is the main CFD software used nowadays for the development and maintenance and launch preparation of the CNES launcher *Ariane5*. It is developed on FORTRAN and uses its own “ghost” environment for the pre-processing, meshing and post-processing tools. It is solving compressible multi-species reacting flows with the fully accounted viscous effects on the unstructured 3D numerical grid. Time splitting is used for the explicit scheme order up to 4 in time and up to 3 in space. The fluxes in the current study are computed on the cell interfaces with HLLC(by Toro) scheme or Roe’s upwind difference splitting scheme for perfect gases. Beside used schemes 10 different schemes may be used for perfect and real gases from HLLc to ASUSM and ASUSM+ and several combustion and kinetic models. In the present study flux vectors are evaluated at each time step using the 2nd order scheme.

To model turbulent flows the 2-equation Jones-Launder k-ε model is used. In the current nozzle study major turbulence effects are concentrated near the nozzle wall and at the separation zone. The CPS includes provisions for modeling the boundary layer flows developing along the walls. In the current study good resolution of numerical grid allowed y^+ values ranging below 11. In the external region where naturally grid is noticeably stretched, the wall function, adiabatic in present case, is used and coupled to the turbulence model by the procedure of modified logarithmic law of Van Driest.

In the current study dry air is used to simulate nozzle flow performance and it is modeled as a perfect gas with power-law expression for $\gamma(T)$ and $C_p(T)$ as a 7th degree polynomials.

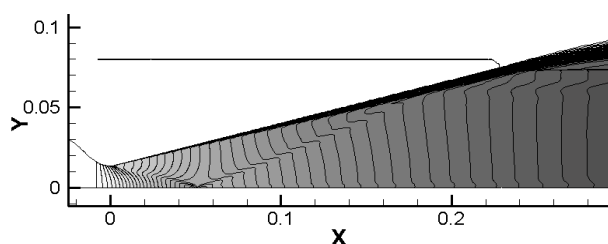


Figure 5. Mach number contours in the conical nozzle at adapted flow regime $NPR=NPR_b$

4. RESULTS AND DISCUSSION

Results presented in the study first are used to identify TIC, Conical and TOC nozzle flow field and their specific properties. Afterwards analysis is coupled in order to describe more complex separation effects.

4.1 Nozzle flow fields

In Figure 5 the adapted dry air flow in the conical nozzle is depicted. After converging section and sonic throat flow expands quasi-equivocally at each portion of the divergent section until it is exhausted at the nozzle exit. It is possible to observe weak compression waves which form in the conical nozzle due to expansion restriction imposed by the nozzle wall. As the flow naturally evolves and expands in the nozzle its expansion to the tangency value at the wall is prevented by the straight oblique profile. As a consequence weak compression waves are generated and they are detectable in any conically profiled nozzle. The magnitude of these waves depends on the flow regime but mainly on the slope of the wall boundary which is defined by the nozzle half-conic angle. For the wide range of launcher nozzle pressure ratios it is found that optimal half-conical angle is around $\sim 15deg$ which is used in this test model also. Weak compression waves are noted to be strengthened at the axis and lessen towards the wall as a consequence of the flow momentum although, their influence on the main flow and separation is not detected.

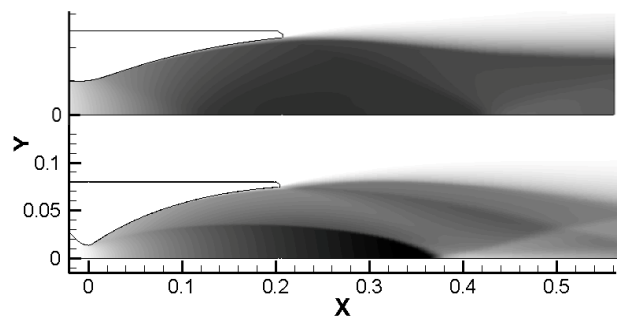


Figure 6. Resulting Mach contour plots of the TIC and TOC nozzles at adapted flow regime $NPR=NPR_b$

In Figure 6 truncated ideal and thrust optimized contour nozzles are shown for adapted flow regime. The previously inviscid MoC calculated profiles are corrected for the BL thickness. The flow in the ideal nozzle expands “perfectly” from the sonic line toward the exit leaving no disturbance or shock wave inside the nozzle. Perfect expansion in the nozzle has its downsides in thickening of the boundary layer towards the exit which decelerates the exhaust plume reducing the delivered thrust and in very long nozzle extension making it for real use impossible.

Compromise is found in truncating the contour leaving the flow at the nozzle exit non-uniform and not fully expanded in all sections but with noticeably shorter divergent length and still no flow deformations or shock waves inside the nozzle. TIC nozzle in the present study had exit angle of $5.4deg$. TIC nozzles are in use on many of the contemporary space launchers as Soyuz RD-0120 or the LE-7 Japanese launcher [6].

In the lower part of Figure 6 TOC nozzle Mach contour plot is shown. The appearance of the internal shock along the nozzle which separates kernel with high momentum flow from the flow that gradually degrades towards the boundary layer (radial gradient) is clearly observable.

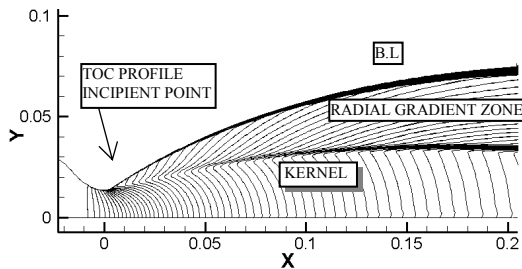


Figure 7. TOC nozzle flow pattern from 2D-axis simulation

Observed from the subsonic part, in order to maximally shorten the nozzle, the curvature radii are small but still deliver flow smoothly the throat. From the end of the sonic line, the emended contour commences with high slope gradient from the supersonic throat curvature portion allowing immense expansion. This represents inflection point in the flow, initiating the internal shock. Nevertheless, high momentum kernel flow allows higher amount of the flow to be expanded and fully accelerated at the exit while on other side of the internal shock, flow gradually evolves towards the wall. This has clear performance increase comparing to the other nozzle configurations. This improved nozzle contour has consequential and complex shock interaction pattern at the overexpanded regime and especially at the engine startup transitional phase.

4.2 Shock structure in overexpanded nozzle flows

At the added external domain in Figure 6, compression sequence out of the nozzle exit is visible. When overexpansion is moderate back pressure imposes adverse gradient to the boundary layer at the nozzle lip and detach it at the exit with the shock surface line under smaller slope towards the axis.

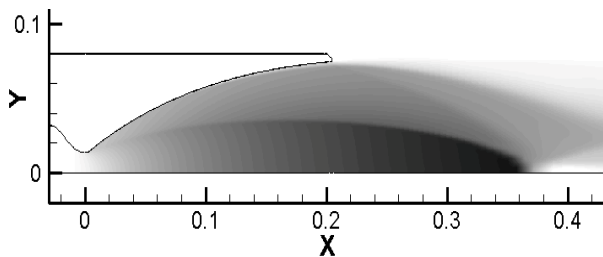


Figure 8. TOC nozzle flow pattern at $p_c/p_a=185$

It is detectable that at this pressure ratio, oblique shock line from the exit propagates to the center line with practically same rate as the main flow at the axis with some strengthening of the compression wave near the axis, which results in the reflection appearing without a Mach disk or so-called regular reflection on the end. This is approximated state and the Mach disk is always present as stronger compression near the axis shows. With the increase of the ambient pressure Mach disk becomes clearly visible, Figure 8.

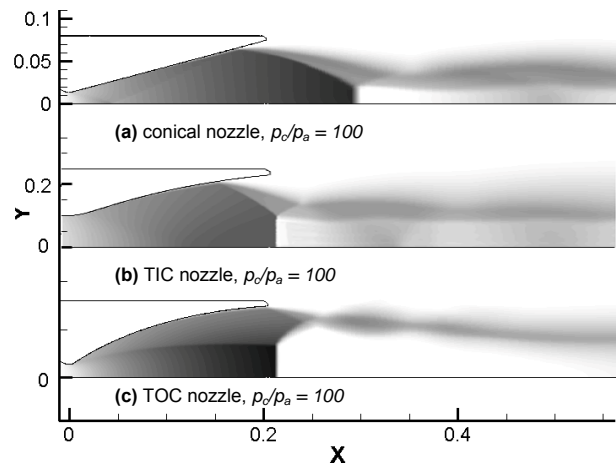


Figure 9. Mach shock patterns of conical, TIC and TOC nozzle at $NPR=100$

For the equally lowered NPR of the conical and TIC nozzle Mach disk augments and drawbacks upstream towards the nozzle exit as depicted in Figure 9 (a) and (b). At the TOC nozzle case (c), as a Mach disk approaches the nozzle with an increase of the ambient pressure the interaction between the internal shock, pressure caused separation and the Mach disk takes place. This inevitably leads to the creation of the cap shock pattern, which appear in the forms as depicted in the previous section. The cap shock pattern, as such is confirmed in number of experiments on full scale and subscale nozzles as reported in [9,10,14-18] and also depicted on Fig 10. Appearance of the cap shock effectively increases pressure behind but also induces very complex shock interaction flowfield, downstream. As this state is usually transitional it tends to oscillate and axially move with the upstream and back pressure fluctuations.

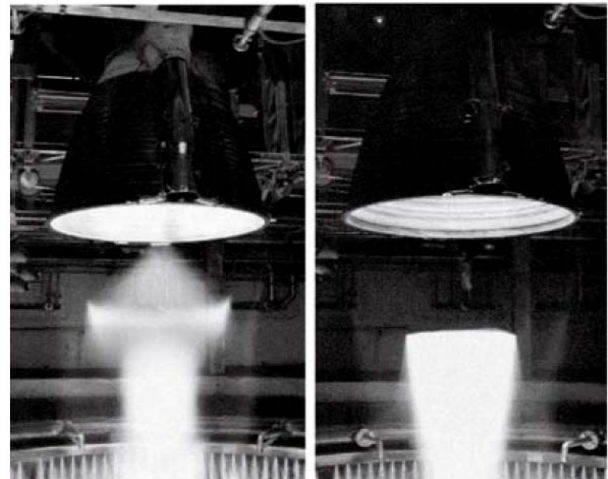


Figure 10. Vulcain nozzle ground testing, (left) cap shock pattern (right) Mach disk reflection by Hagemann & Frey [6]

In Figure 10 photos of Vulcain nozzle test reported by Hagemann and Frey [6] are shown. The cap-shock on the left and Mach disk reflection on the right depict transitional stage during start-up and shut down operation as the critical phases of the engine operation. Unsteadiness that may occur during these phases may impose lethal lateral loads on the nozzle and engine structure and jeopardize complete launch sequence as reported in [4,15].

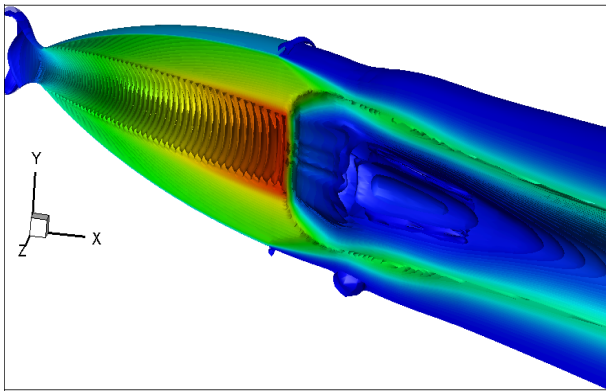


Figure 11. Cap-shock shown with 3D numerical Mach iso-surfaces for $NPR=100$

Iso-Mach surfaces extracted from numerical simulation results depict structure of the cap-shock nozzle flow pattern. Figure 11. Internal shock, normal Mach disk and reflected separation shock meet at the triple point after which internal shock and separation interact and reflect creating the truncated-cone shaped compression sequence. Selected streamlines $\Phi 1$ and $\Phi 2$ above and below triple point are further analyzed in the shock polar diagram for the flow deflection – pressure relation.

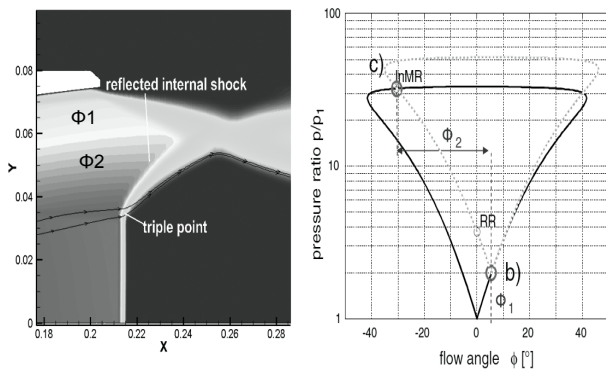


Figure 12. cap-shock section and shock polar plane for 2 streamlines $\Phi 1$ and $\Phi 2$

4.3 Nozzle flow separation patterns

As the NPR decreases the separation and the cap shock enter the nozzle extension region. Hagemann and Frey [4] related this directly to the occurrence of RSS and FSS/RSS transition as the inviscid mechanism contrary to some other assumptions. Namely, the propagation of the reflected or triple shock originating from the triple point at the tip of cap shock limits/restricts the free shock separation extension and as a consequence the flow reattaches downstream to the wall. In the current test case for the pressure ratios between $NPR=50$ and $NPR=40$ both patterns were possible and unsteady. In Figure 13 FSS is captured with a higher side tilted towards the wall. With further NPR decrease qRSS goes to RSS. RSS depicted Figure 14 imposes recirculation zones between separation and reattachment points at the wall. In the main flow trapped vortex or counter rotating vortex pair is formed being trapped inside the sequence region between cap shock and the end. Vortex motion inside allows “breathing” of the trapped flow which is by number of authors related [16,19] to FSS/RSS transition and oscillations.

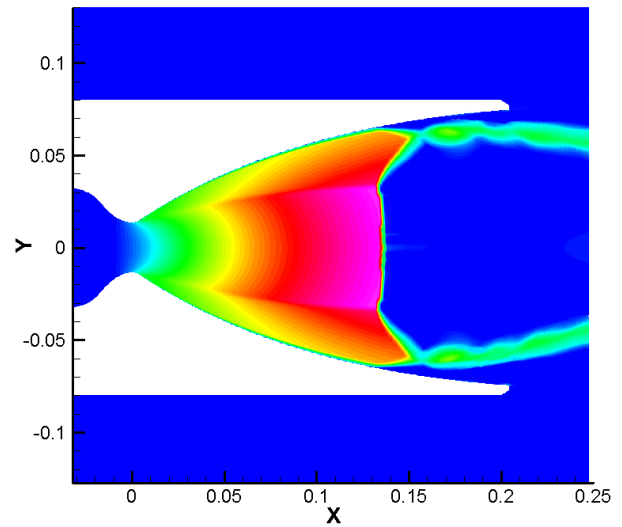


Figure 13. Mach plot at normal plane depicting Free Shock Separation FSS at $NPR=40$

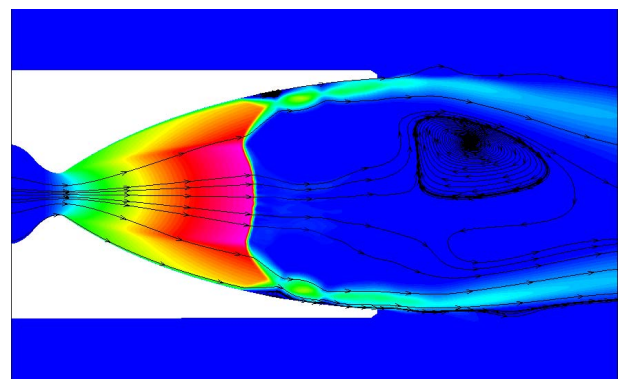


Figure 14. Mach plot at normal plane depicting Restricted Shock Separation RSS at $NPR=30$

The recirculation formed near the wall effectively controls the pressure imposed on the wall. For the FSS, flow separates due to adverse pressure gradient and the back flow enters the nozzle rapidly increasing the pressure as the back flow turns and forms long loop the slope of the pressure profile starts to decrease going to its plateau ambient value.

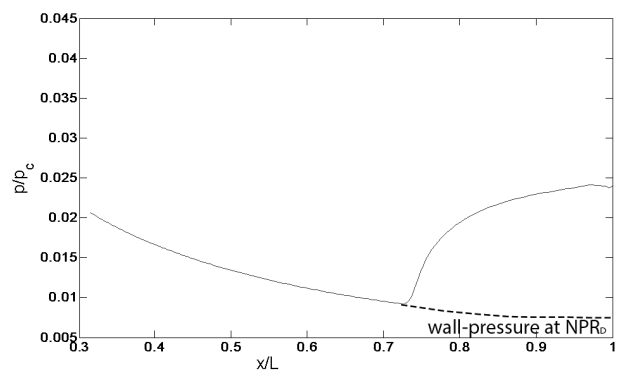


Figure 15. FSS - dimensionless wall pressure profile

At RSS case in Figure 16, flow separates with rapid pressure increase to the plateau value. As it is reached, flow is being pulled and reattached to the wall again resulting in the pressure peak.

After impacting the wall flow is detached again but with very short separated length and counter-rotating recirculation. Shortly after flow is being reattached to the wall resulting in the next pressure peak, observable

in the pressure plot paired with the contour plot in Figure 16. With degradation of the separated flow momentum the RSS continues with reduced intensity. In Figure 17 wall pressure profiles of the five different pressure ratios are depicted. As assumed, the maximum relative pressure value is reached for the lowest NPR=10 analogous to the startup operation sequence. Next pressure peak is reached for the highest NPR=50 depicting the transition and nozzle end-effect. As such, analysis of FSS/RSS represents one of the absolute design criteria for the modern launcher engine nozzles.

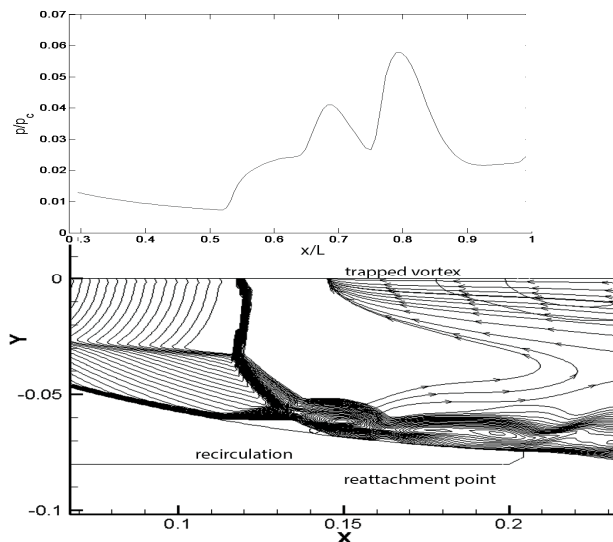


Figure 16. RSS - dimensionless wall pressure profile

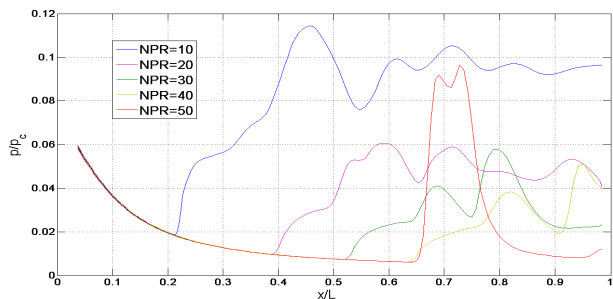


Figure 17. wall-pressure profiles for RSS at different NPR hysteresis regimes

The RSS, partial pRSS and quasi qRSS states are found to be highly unsteady causing the asymmetric reattachments along the nozzle extension wall. Although observed and registered in a number of tests, the causes and mechanism of this flow unsteadiness are still not completely understood. Several theories based on the observation reasoning emerged about driving, physical mechanisms as, for example, Smits and Dussauge [20] who suggested the flow over the separated zone, being sensitive to compression effects, imposes unsteady conditions on the shock and makes it to move. More accepted was the reasoning that the flow unsteadiness is caused by the mass imbalance of reversed fluid flow at the reattachment point to that scavenged from the separation point and is responsible for the breathing motion of the separation bubble. It is noted that the model of mass-exchange appears to yield more accurate semi-empirical correlations as reported by Verma [15].

Numerical methods used in this study were based on the RANS and FANS compressible solvers. The averaging numerical approach tends to flatten unsteady part of the flow. In order to numerically investigate the inflicted instabilities and causes more direct method would be appropriate. LES (large eddy simulation) method is still not adapted to high speed internal supersonic flows implementation and regions close to the wall and its computation cost for such a case still represents the problem. Development of hybrid RANS/LES methods for supersonic flows, namely from Spalart-Allmaras based DES (detached eddy simulation) have increased attention in numerical field of nozzle investigation. In the mentioned model one-equation turbulence model is used to solve eddy viscosity in BL region and LES is solving eddies in free stream region (detached eddies). Nevertheless, due to the problems of matching viscosity term with deformation term in the zone between BL and free stream and due to appearance of numerically induced viscos diffusivity Deck [21], [22] has proposed used of zonal DES, ZDESin which RANS and DES domains are selected individually. This method has been successfully used in a number of applications. Spalart proposed modification of wall distance term presented as delayed detached eddy simulation DDES which is adapted to the nozzle investigation as reported by Deck [23].

5. CONCLUDING REMARKS

In the current study basic flow patterns that appear under overexpanded flow conditions in supersonic axisymmetric propulsive nozzles are described and analyzed. Literature rendering of fundamental and advanced nozzle investigation methods is briefly exposed. Conical and TIC nozzle are designed using the method of characteristics and compared with the TOC nozzle configuration. Using the cold flow RANS/FANS numerical approach of two major European solvers, elsA and CPS, flow under various overexpanded pressure ratios is simulated and analyzed. Cap-shock pattern, transition FSS/RSS and RSS are analyzed and presented from extracted numerical results that were excellent corresponded to previous experiments and reported works. Design criteria for rocket nozzles may be given considering reported results. Additional work on instabilities, understanding of the causes and methods to prevent critical loads on certain operation points is needed and is investigation point in number of research teams.

ACKNOWLEDGMENT

To Sébastien Deck from ONERA for the provided data and guidance during the MEC 578 student project and to professor Denis Sipp (Ecole Polytechnique and ONERA) for the course supervision.

REFERENCES

- [1] Hoffman, J.D.: *Optimum Thrust Nozzle Contours for Chemically Reacting Gas Flows*, NASA Report TM-66-3, 1966.

- [2] Hadjadj, A. and Onofri, M.: Nozzle flow separation, *Shock Waves J.*, Vol. 19, No.3, pp. 163-169, 2009.
- [3] Nave, L.H., Coffey, G.A.: Sea level side loads in high-area-ratio rocket engines. AIAA Paper 73-1284, 9th AIAASAE Propulsion Conference
- [4] Frey, M. and Hagemann, G.: Restricted shock separation in rocket nozzles. AIAA J. of Propulsion and Power, Vol.16, No.3, pp. 478-484, 2000.
- [5] Hagemann, G., Frey, M. and Koschel W.: Appearance of restricted shock separation in rocket nozzles, AIAA J. of Propulsion and Power, Vol. 18, No. 3, pp. 577-584, 2002.
- [6] Hagemann, G. and Frey, M.: Shock pattern in the plume of rocket nozzles: needs for design consideration, *Shock Waves J.*, Vol. 17, No.2, pp. 387-395, 2008.
- [7] Deck, S. and Nguyen, A.T.: Unsteady side loads in a Thrust-Optimized Contour nozzle at hysteresis regime, AIAA J., Vol. 42, No. 9, pp. 1878-1888, 2004.
- [8] Reijasse P. and Poutrel, R.: Flow separation regimes induced by cap-shock in over-expanded optimized propulsive nozzles, in: *Proceedings of the EUCASS*, 2005, Moscow, pp. 1-8.
- [9] Shimizu, T., Kodera, m. and Tsuboi, N.: Internal and external flow of rocket nozzle, *J. of the earth Simulator*, Vol.9, pp. 19-26, 2008.
- [10] Roquefort, T.A.: Unsteadiness and side loads in over-expanded supersonic nozzles, in: *Proceedings of the ESA Symposium Aerothermodynamics for Space Applications*, 15-18 Oct. 2001, Capua, Italy, ESA SP-487, pp. 93-107.
- [11] Rao, G.V.R.: Exhaust nozzle contour for optimum thrust. *Jet Propulsion J.*, Vol.28, 377382, 1958.
- [12] Cambier, L. and Gazaix, M: elsA: an efficient object-oriented solution to CFD complexity, in: *AIAA ASME*, 14-17 Jan. 2002, Reno, USA, AIAA 2002-0108.
- [13] Durand P., Vieille B, Lambare H, Vuillermoz P, Boure G, Steinfeld P, Godfroy F, and Guery J.F.: CPS: A three-dimensional CFD numerical code dedicated to space propulsive flows, AIAA Paper A00-36976 3864, 2000.
- [14] Vuillermoz, P., Lambare, H., Enzian, A., Steinfeld, P. and Lequette, L.: Computational flow simulations of overexpanded rocket nozzle flowfields including unsteady effects, in: *Proceedings of the ESA Symposium Aerothermodynamics for Space Applications*, 15-18 Oct. 2001, Capua, Italy, ESA SP-487 pp. 391-398.
- [15] Verma S.B.: Shock unsteadiness in a thrust optimized parabolic nozzle, *Shock Waves J.*, Vol. 19, No.3, pp. 193-212, 2009.
- [16] Nasuti, F. and Onofri, M.: Shock structure in separated nozzle flows, *Shock Waves J.*, Vol. 19, No.3, pp. 229-237, 2009.
- [17] Chpoun, A. and Leclerc, E.: Experimental investigation of the influence of downstream flow conditions on Mach stem height, *Shock Waves* 9, pp. 269-71, 1999.
- [18] Chpoun, A., Passerel, D., Li, H., and Ben-Dor, G.: Reconsideration of oblique shock wave reflection in steady flows, *J. Fluid. Mech.* 1995. Vol. 301, pp. 19-35.
- [19] Martelli, E., Nasuti F. and Onofri, M.: Numerical calculation of FSS/RSS transition in highly overexpanded rocket nozzle flows, *Shock Waves J.*, Vol. 20, No.1, pp. 139-146, 2010.
- [20] Smits, A. and Dussauge, J.P.: *Turbulent Shear Layers in Supersonic Flow*. AIP press, 2006.
- [21] Deck, S. and Thorigny, P.: Unsteadiness of an axisymmetric separating-reattaching flow, *AIP Physics of Fluids J.*, Vol. 19, 065103, 2007.
- [22] Deck, S.: Zonal-detached eddy simulation of the flow around a high-lift configuration. AIAA J. Vol. 4, No. 11, pp. 2372-2384, 2005.
- [23] Deck, S.: Delayed detached eddy simulation of the end-effect regime and side-loads in an overexpanded nozzle flow, *Shock Waves J.*, Vol. 19, No. 3, pp. 239-249, 2009.

ТИПОВИ ОДВОЈЕНОГ СТРУЈАЊА И БОЧНИ ФЕНОМЕНИ У СУПЕРСОНИЧНОМ РАКЕТНОМ МЛАЗНИКУ

Владета Змијановић, Бошко Рашуо, Амер Шпун

Феномени одвојеног струјања који се јављају у конвергентно-дивергентном млазнику при надекспанираним условима су описани и испитани. Овај режим рада млазника је нарочито изражен код модерних свемирских лансера чији млазници имају веома широку анвелопу рада. Поред убичајених проблема надекспанираног млазника код модерних потисно оптимизованих млазника се јавља додатни проблем услед саме геометрије – профила млазника. Наиме, оптимизовањем идеалне де Лавалове контуре добијени профил одступа од идеалне експанзије. Као одговор на ову деформацију јавља се унутрашњи ударни талас унутар млазника. При оптималним условима ово је жељени ефекат јер се млаз у млазнику дели на језгро великог импулса и бочно-радијално струјање. Међутим при условима на полетању или при старту мотора интеракција ударних таласа и Маховог диска ствара каполики тип рекомпресије који аксијално пулсира и на крају доводи до рестриктивног одвајања у млазнику. Овај тип одвајања је веома нестабилан и опасан и евентуално, може потпуно оштети или уништити ракетни мотор. У овом истраживању су коришћене нумеричке методе и кодови елса и ЦПС који се тренутно користе при дизајнирању режима полетања европског тешког лансера Ариане 5.